these glial markers during this peak period of gliogenesis, confirming that Dcx is expressed solely in immature neurons.

Microscopy

We performed confocal microscopy using a Noran Instruments Oz Confocal Laser Scanning Microscope, a Nikon Diaphot optical microscope, and Intervision 3D analysis software. We produced 3D digital reconstructions from a series of confocal images taken at 0.3 or 0.5 μm intervals through the region of interest. This 3D analysis allowed us unequivocally to co-localize BrdU and markers of differentiation. We compiled the montage in Fig. 1f from three sequential sections from the anterior forebrain of an experimental 28-week-survival mouse.

Quantification

We quantified the number of BrdU+ cells and BrdU+/NeuN+ neurons in experimental and control regions by sampling every sixth section, using a modified version of the fractionator method[31]. The experimental regions of cortex extended from dorsal cortex to the medial bank, and spanned the thickness of cortical layer VI. We compared numbers of new neurons in experimental mice to control mice by multiple statistical methods: unpaired two-tailed *t* test; non-parametric two-tailed Mann–Whitney test; and unpaired *t*-test with Welch correction. All methods yielded *P* values less than 0.0009, demonstrating a highly significant difference between the groups.

FluoroGold Injections

We stereotactically injected 32 nl of 3% FluoroGold solution dissolved in water bilaterally at each of the same three thalamic sites as the original nanosphere injections. We injected the retrograde label FluoroGold into the thalamus of adult mice eight weeks after induction of targeted corticothalamic neuron apoptosis, and perfused the mice at nine weeks.

Received 11 January; 3 May 2000.

1. Altman, J. & Das, G. D. Autoradiographic and histological evidence of postnatal hippocampal neurogenesis in rats. *J. Comp. Neurol.* **124,** 319–335 (1965).
2. Altman, J. Autoradiographic and histological studies of postnatal neurogenesis. IV. Cell proliferation and migration in the anterior forebrain, with special reference to persisting neurogenesis in the olfactory bulb. *J. Comp. Neurol.* **137,** 433–457 (1969).
3. Luskin, M. B. Restricted proliferation and migration of postnatally generated neurons derived from the forebrain subventricular zone. *Neuron* **11,** 173–189 (1993).
4. Lois, C. & Alvarez-Buylla, A. Proliferating subventricular zone cells in the adult mammalian forebrain can differentiate into neurons and glia. *Proc. Natl Acad. Sci. USA* **90,** 2074–2077 (1993).
5. Kaplan, M. S. & Hinds, J. W. Neurogenesis in the adult rat: electron microscopic analysis of light radioautographs. *Science* **197,** 1092–1094 (1977).
6. Gould, E., Reeves, A. J., Graziano, M. S. A. & Gross, C. G. Neurogenesis in the neocortex of adult primates. *Science* **286,** 548–552 (1999).
7. Macklis, J. D. Transplanted neocortical neurons migrate selectively into regions of neuronal degeneration produced by chromophore-targeted laser photolysis. *J. Neurosci.* **13,** 3848–3863 (1993).
8. Sheen, V. L. & Macklis, J. D. Targeted neocortical cell death in adult mice guides migration and differentiation of transplanted embryonic neurons. *J. Neurosci.* **15,** 8378–8392 (1995).
9. Gleeson, J. G., Lin, P. T., Flanagan, L. A. & Walsh, C. A. Doublecortin is a microtubule-associated protein and is expressed widely by migrating neurons. *Neuron* **23,** 257–271 (1999).
10. Francis, F. *et al.* Doublecortin is a developmentally regulated, microtubule-associated protein expressed in migrating and differentiating neurons. *Neuron* **23,** 247–256 (1999).
11. Marusich, M. F., Furneaux, H. M., Henion, P. D. & Weston, J. A. Hu neuronal proteins are expressed in proliferating neurogenic cells. *J. Neurobiol* **25,** 143–155 (1994).
12. Barami, K., Iversen, K., Furneaux, H. & Goldman, S. A. Hu protein as an early marker of neuronal phenotypic differentiation by subependymal zone cells of the adult songbird forebrain. *J. Neurobiol.* **28,** 82–101 (1995).
13. Reh, T. A. Cell-specific regulation of neuronal production in the larval frog retina. *J. Neurosci.* **7,** 3317–3324 (1987).
14. Parent, J. M. *et al.* Dentate granule cell neurogenesis is increased by seizures and contributes to aberrant network reorganization in the adult rat hippocampus. *J. Neurosci.* **17,** 3727–3738 (1997).
15. Snyder, E. Y., Yoon, C., Flax, J. D. & Macklis, J. D. Multipotent neural precursors can differentiate toward replacement of neurons undergoing targeted apoptotic degeneration in adult mouse neocortex. *Proc. Natl Acad. Sci. USA* **94,** 11663–11668 (1997).
16. Kirn, J. R. & Nottebohm, F. Direct evidence for loss and replacement of projection neurons in adult canary brain. *J. Neurosci.* **13,** 1654–1663 (1993).
17. Gould, E. & Cameron, H. A. Regulation of neuronal birth, migration and death in the rat dentate gyrus. *Dev. Neurosci.* **18,** 22–35 (1996).
18. Wang, Y., Sheen, V. L. & Macklis, J. D. Cortical interneurons upregulate neurotrophins *in vivo* in response to targeted apoptotic degeneration of neighboring pyramidal neurons. *Exp. Neurol.* **154,** 389–402 (1998).
19. Hernit-Grant, C. S. & Macklis, J. D. Embryonic neurons transplanted to regions of targeted photolytic cell death in adult mouse somatosensory cortex re-form specific callosal projections. *Exp. Neurol.* **139,** 131–142 (1996).
20. Shin, J. S. Transplanted neuroblasts differentiate appropriately into projection neurons with the correct neurotransmitter and receptor phenotype in neocortex undergoing targeted projection neuron neurodegeneration. *J. Neurosci.* (in the press).
21. Scharff, C. *et al.* Targeted neuronal death affects neuronal replacement and vocal behavior in adult songbirds. *Neuron* **25,** 481–492 (2000).
22. Palmer, T. D. *et al.* Fibroblast growth factor-2 activates a latent neurogenic program in neural stem cells from diverse regions of the adult CNS. *J. Neurosci.* **19,** 8487–8497 (1999).
23. Reynolds, B. A. & Weiss, S. Generation of neurons and astrocytes from isolated cells of the adult mammalian central nervous system. *Science* **255,** 1707–1710 (1992).
24. Richards, L. J., Kilpatrick, T. J. & Bartlett, P. F. *De novo* generation of neuronal cells from the adult mouse brain. *Proc. Natl Acad. Sci. USA* **89,** 8591–8595 (1992).
25. Vescovi, A. L., Reynolds, B. A., Fraser, D. D. & Weiss, S. bFGF regulates the proliferative fate of unipotent (neuronal) and bipotent (neuronal/astroglial) EGF-generated CNS progenitor cells. *Neuron* **11,** 951–966 (1993).
26. Morshead, C. M. *et al.* Neural stem cells in the adult mammalian forebrain: a relatively quiescent subpopulation of subependymal cells. *Neuron* **13,** 1071–1082 (1994).
27. Craig, C. G. *et al. In vivo* growth factor expansion of endogenous subependymal neural precursor cell populations in the adult mouse brain. *J. Neurosci.* **16,** 2649–2658 (1996).
28. Kuhn, H. G. *et al.* Epidermal growth factor and fibroblast growth factor-2 have different effects on neural progenitors in the adult rat brain. *J. Neurosci.* **17,** 5820–5829 (1997).
29. Zigova, T., Pencea, V., Wiegand, S. J. & Luskin, M. B. Intraventricular administration of BDNF increases the number of newly generated neurons in the adult olfactory bulb. *Mol. Cell. Neurosci.* **11,** 234–245 (1998).
30. Cameron, H. A., Hazel, T. G. & McKay, R. D. Regulation of neurogenesis by growth factors and neurotransmitters. *J. Neurobiol.* **36,** 287–306 (1998).
31. Guillery, R. W. & Herrup, K. Quantification without pontification: choosing a method for counting objects in sectioned tissues. *J. Comp. Neurol.* **386,** 2–7 (1997).

Acknowledgements

We thank J. Gleeson, S. Goldman, M. Marusich, C. Walsh, and P. Follett for reagents; M. Christian and C. Tai for technical assistance; L. Catapano, P. Follett, R. Fricker, M. Gates, and J. Gleeson for discussions; and L. Benowitz, M. Greenberg, L. Kunkel, and C. Walsh for critical reading. This work was supported by grants from the NIH (J.D.M.), Alzheimer's Association (J.D.M.), Human Frontiers Science Program (J.D.M.), an NIH predoctoral training grant (S.S.M.), and a postdoctoral fellowship from the Canadian MRC (B.R.L.).

Correspondence and requests for materials should be addressed to J.D.M. (e-mail: macklis@hub.tch.harvard.edu).

Regulation of distinct AMPA receptor phosphorylation sites during bidirectional synaptic plasticity

Hey-Kyoung Lee*, Michaela Barbarosie†, Kimihiko Kameyama‡, Mark F. Bear† & Richard L. Huganir*

** Howard Hughes Medical Institute, Department of Neuroscience, Johns Hopkins Medical School, Baltimore, Maryland 1205, USA*
† Howard Hughes Medical Institute, Department of Neuroscience, Brown University, Providence, Richmond 02912, USA
‡ Laboratory of Molecular Neurobiology, National Institute of Bioscience and Human Technology, Ibaraki 305-8566, Japan

Bidirectional changes in the efficacy of neuronal synaptic transmission, such as hippocampal long-term potentiation (LTP) and long-term depression (LTD), are thought to be mechanisms for information storage in the brain[1–4]. LTP and LTD may be mediated by the modulation of AMPA (α-amino-3-hydroxy-5-methyl-4-isoxazloe proprionic acid) receptor phosphorylation[5–7]. Here we show that LTP and LTD reversibly modify the phosphorylation of the AMPA receptor GluR1 subunit. However, contrary to the hypothesis that LTP and LTD are the functional inverse of each other, we find that they are associated with phosphorylation and dephosphorylation, respectively, of distinct GluR1 phosphorylation sites. Moreover, the site modulated depends on the stimulation history of the synapse. LTD induction in naive synapses dephosphorylates the major cyclic-AMP-dependent protein kinase (PKA) site, whereas in potentiated synapses the major calcium/calmodulin-dependent protein kinase II (CaMKII) site is dephosphorylated. Conversely, LTP induction in naive synapses and depressed synapses increases phosphorylation of the CaMKII site and the PKA site, respectively. LTP is differentially sensitive to CaMKII and PKA inhibitors depending on the history of the synapse. These results indicate that AMPA receptor phosphorylation is critical for synaptic plasticity, and that identical stimula-

tion conditions recruit different signal-transduction pathways depending on synaptic history.

AMPA receptors, the principal excitatory neurotransmitter receptors in the brain, are composed of four different subunits (GluR1–4) that can assemble in different combinations[8,9]. The GluR1 subunit is predominantly expressed in the forebrain, including the hippocampus, a region implicated in memory formation[10]. A study using GluR1 knockout mice has shown that this subunit is essential for LTP in the CA1 region of the adult hippocampus[11]. The GluR1 subunit is regulated by protein phosphorylation at two sites on its intracellular carboxy-terminal domain[12]. Serine 831 is phosphorylated by CaMKII and protein kinase C (PKC), whereas serine 845 is phosphorylated by PKA[12–14]. Phosphorylation of either of these sites potentiates AMPA receptor function through distinct biophysical mechanisms[12,13,15,16].

The aim of this study was to examine changes in phosphorylation of GluR1 at these two sites after the synaptic induction of LTP and LTD using phosphorylation-site-specific antibodies. A chemically induced form of LTD (chemLTD) is associated with persistent dephosphorylation of GluR1 at a PKA phosphorylation site, Ser 845 (refs 6, 7). The chemLTD approach was designed to maximize the number of affected synapses, thereby increasing the probability of detecting biochemical changes. We have been able to increase the sensitivity of our assay to detect small changes in GluR1 phosphorylation on Ser 831 and Ser 845 in single hippocampal slices after the synaptic induction of LTP and LTD.

To analyse phosphorylation of GluR1 during synaptic plasticity, we placed two hippocampal slices in the same recording chamber and recorded extracellular field potentials simultaneously in the CA1 dendritic region of both slices upon stimulation of the Schaffer collaterals. After collecting a stable baseline, stimulation to one slice was turned off while the other slice received low-frequency stimulation (LFS; 1 Hz, 900 pulses). After the LFS, the stimulation was returned to the baseline frequency, and stimulation to the control slice was resumed. The slice that received LFS showed homosynaptic LTD (78 ± 3% of baseline field potential slope 1 h after the onset of 1-Hz stimulation, $n = 17$), but there was no significant change in synaptic strength in the control slice (101 ± 2% of baseline, $n = 17$; Fig. 1a). One hour after the induction of LTD the slices were collected and frozen immediately on dry ice. We then analysed the phosphorylation states of GluR1 at Ser 831 and Ser 845 in the control and LTD slices by quantitative immunoblotting.

Like chemLTD, homosynaptic LTD produced specific dephosphorylation of Ser 845 (87 ± 3% phosphorylation of control slices, $n = 17$; paired t-test: $P < 0.01$; Fig. 1c), whereas there was no significant change in phosphorylation of Ser 831 (99 ± 6% of control; Fig. 1b and c). The dephosphorylation at Ser 845 could be detected as early as 30 min after the onset of LFS (83 ± 5% of control, $n = 11$; Fig. 1c). As expected, the magnitude of the change in GluR1 phosphorylation following homosynaptic LTD was smaller than that reported for chemLTD, because only a small percentage of synapses in the slice are depressed during LFS-induced homosynaptic LTD. This effect was, however, reproducible and statistically significant. In addition, there was no dephosphorylation in slices that did not exhibit LTD after LFS, either because induction of LTD failed or because the NMDA (*N*-methyl-D-aspartate) receptor antagonist AP5 (D(-)-2-amino-5-phosphonovaleric acid) was

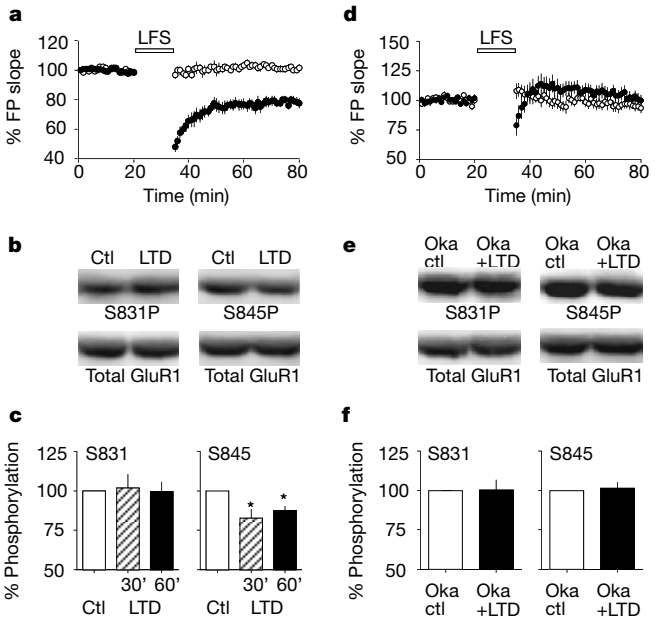

Figure 1 Homosynaptic LTD in CA1 is associated with dephosphorylation of GluR1 at a PKA site. **a**, Simultaneous recording of slices receiving baseline stimulation (control, open circles) and 1-Hz stimulation (LTD, closed circles; $n = 17$ each). FP, field potential. **b**, Immunoblot using antibody against phosphorylated Ser 831 (CaMKII site; S831P) and phosphorylated Ser 845 (PKA site; S845P) on GluR1. Both blots were stripped and reprobed with the antibody recognizing the C-terminal end of GluR1 (total GluR1). **c**, Summary of phosphorylation changes in Ser 831 and Ser 845 following LTD induction 30 min ($n = 11$) and 1 h ($n = 17$) after LFS. Asterisks indicate value statistically significantly different from control. **d**, Homosynaptic LTD is blocked by pretreatment of slices with okadaic acid (control slices: Oka ctl, open circles; LTD slices: Oka+LTD, filled circles; $n = 11$ each). **e**, Immunoblot of slices pretreated with okadaic acid using phosphorylation-site-specific antibodies. Panels as in **b**. Okadaic acid pretreatment increased the phosphorylation of Ser 831 by 155 ± 17% and Ser 845 by 139 ± 24%. **f**, Okadaic acid pretreatment prevented the dephosphorylation of Ser 845 (PKA site) associated with homosynaptic LTD. The signals were normalized as described in **c**.

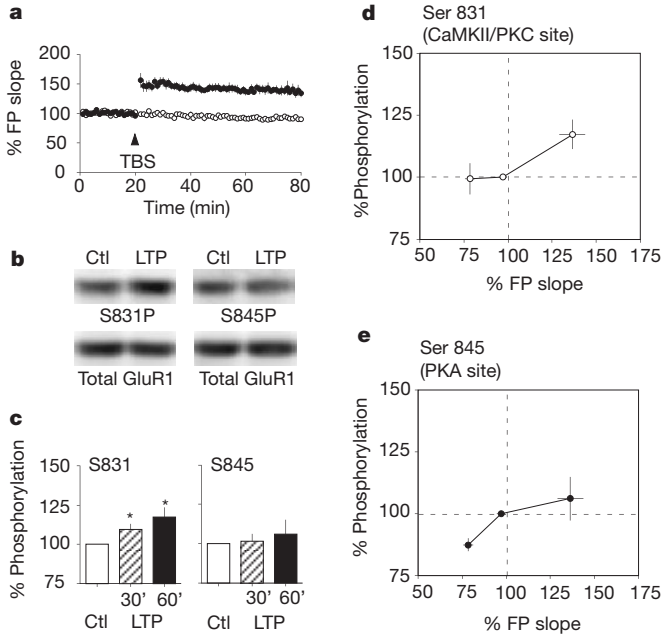

Figure 2 LTP induction increases phosphorylation at CaMKII phosphorylation site on GluR1. **a**, Simultaneous recording of field potentials in control slices (open circles) and LTP slices (closed circles; $n = 13$ each). **b**, Immunoblots using phosphorylation-site-specific antibodies. Panels as in Fig. 1b. **c**, Quantification of immunoblots with samples from control slices (Ctl) and 30 min ($n = 9$) and 1 h ($n = 13$) after LTP induction. One data point was excluded from analysis, as the phosphorylation changes in Ser 845 exceeded 2 s.d. from the mean. The inclusion of this data point does not change the conclusions. **d**, Changes in phosphorylation of GluR1 at the CaMKII site (S831) 1 h after induction of LTP and LTD. **e**, GluR1 phosphorylation changes at the PKA site (S845) associated with bidirectional synaptic plasticity 1 h after induction.

applied (data not shown). Collectively, these results confirm that chemLTD and homosynaptic LTD share similar downstream expression mechanism(s)[6].

Homosynaptic LTD is dependent on postsynaptic protein phosphatase activity[17,18]. To test whether the dephosphorylation of GluR1 following LTD is also sensitive to protein phosphatase inhibitors, we incubated the control and experimental slices in okadaic acid (1 μM in ACSF with 0.1% dimethyl sulphoxide (DMSO)) for 2–3 h and transferred them to the recording chamber. As reported, okadaic acid abolished LTD (101 ± 4% of baseline, $n = 11$, Fig. 1d; LTD in vehicle solution: 76 ± 5%, $n = 10$, data combined in Fig. 1a; t-test, $P < 0.01$). Moreover, pretreatment of slices with okadaic acid blocked the LFS-induced dephosphorylation of Ser 845 (101 ± 7% of OKA controls; $n = 11$; Fig. 1e and f). In contrast, induction of LTD in slices kept in vehicle solution still produced significant dephosphorylation at Ser 845 (88 ± 3% of controls; $n = 10$; paired t-test, $P < 0.05$; data combined in Fig. 1c). This result indicates that protein phosphatase 1/2A may be critical for the LFS-induced dephosphorylation of GluR1 at Ser 845.

LTP is probably associated with an increase in phosphorylation of GluR1 by CaMKII (ref. 5). We tested whether we could detect the same changes using our phosphorylation-site-specific antibodies. Slices that received theta burst stimulation (TBS) showed LTP (134 ± 3% of baseline at 1 h after TBS, $n = 14$; Fig. 2a), and a significant increase in GluR1 phosphorylation at Ser 831 (CaMKII/PKC site) at both 30 min (110 ± 3% of controls, $n = 9$; paired t-test, $P < 0.05$) and 1 h (117 ± 5% of controls, $n = 14$; paired t-test, $P < 0.05$; Fig. 2c) after TBS. Phosphorylation of Ser 845 (PKA site) was not significantly increased 30 or 60 min after LTP induction (Fig. 2b and c). In slices that did not exhibit LTP, GluR1 phosphorylation did not change (data not shown). These results agree with those of previous studies indicating that the early phase of LTP is dependent on postsynaptic CaMKII activation[19,22] and that phosphorylation of GluR1 by CaMKII increases following LTP[5].

The data presented so far indicate that LTP and LTD may be associated with changes in phosphorylation of GluR1 at different sites (Fig. 2d and e). LTD is associated with dephosphorylation at Ser 845, a PKA site, whereas LTP is associated with increased phosphorylation of Ser 831, a CaMKII site. This indicates that although induction of LTP and LTD results in the bidirectional control of AMPA-receptor phosphorylation, LTP and LTD do not regulate phosphorylation of the same site. As LTP and LTD are reversible processes, we tested what happens to GluR1 phosphorylation after the reversal of LTP with LFS ('depotentiation') and the reversal of LTD with TBS ('de-depression').

To examine depotentiation we subjected both slices in the recording chamber to TBS simultaneously, which resulted in LTP. After 30 min of recording, LFS was given to one of the slices. This stimulation depressed the synaptic strength back to the baseline level (depotentiation; 93 ± 4% of baseline 30 min after onset of 1-Hz stimulation, $n = 14$; Fig. 3a) while the synaptic response stayed potentiated in slices that only received TBS (139 ± 3% of baseline at 1 h post-TBS; Fig. 3a). There was significant dephosphorylation of Ser 831 in depotentiated slices (89 ± 5% of LTP slices, $n = 14$: paired t-test: $P < 0.05$) but no significant change in Ser 845 (106 ± 5% of LTP slices; Fig. 3b and c). This result indicates that the same stimulation protocol (LFS) results in the dephosphorylation of different sites on GluR1 depending on the previous experience of the synapse (whether it had previously undergone LTP).

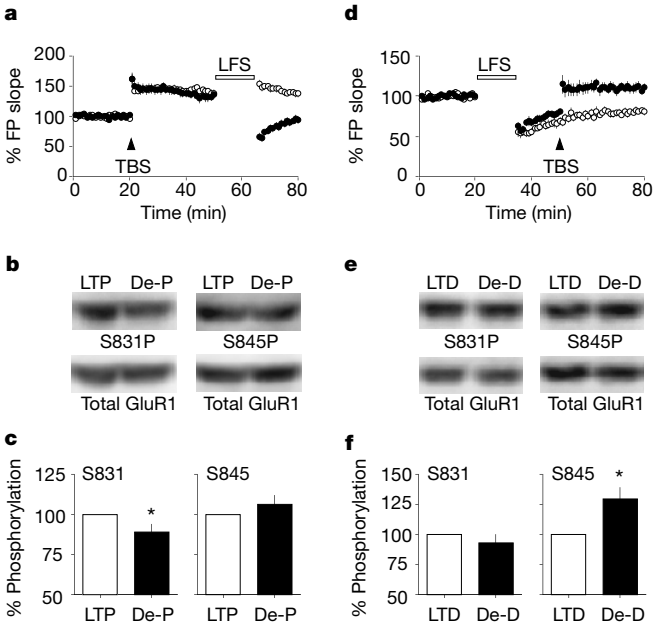

Figure 3 Depotentiation results in dephosphorylation of a CaMKII site on GluR1, whereas de-depression is associated with an increase in phosphorylation of a PKA site. **a**, To detect changes associated with depotentiation (De-P, closed circles), we compared it with LTP (open circles; $n = 14$ each). **b**, Representative immunoblots of LTP and depotentiation (De-P) samples. Panels as in Fig. 1b. **c**, Depotentiation dephosphorylates Ser 831 (CaMKII site). Open bars, phosphorylation levels in LTP slices; closed bars, per cent phosphorylation in depotentiation slices (De-P; $n = 14$ each). **d**, De-depression (De-D, closed circles) was tested against LTD (open circles; $n = 10$ each). **e**, Immunoblots of LTD and de-depression (De-D) slices. **f**, De-depression increases phosphorylation at Ser 845 (PKA site).

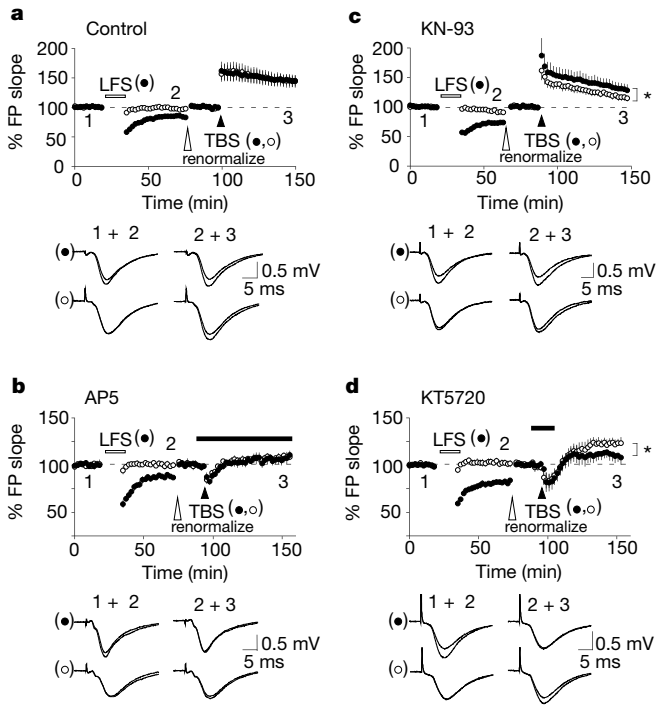

Figure 4 De-depression and LTP utilize different signal transduction pathways for their expression. **a**, De-depression (closed circles) and LTP (open circles) in normal ACSF ($n = 11$) in a two-pathway experiment. Sample field potential responses from one experiment taken at time points indicated are shown below. **b**, Both de-depression (closed symbols) and LTP (open symbols) are blocked by DL-AP5 (100 μM; $n = 4$). Below, field potential recordings from a typical experiment. **c**, The CaMKII inhibitor KN93 affects LTP (open circles) more than de-depression (closed circles; $n = 8$). Below, examples of field potential responses from one experiment. **d**, PKA inhibitor KT5720 reduced de-depression (closed circles) more than LTP (open circles; $n = 6$). KT5720 (1 μM) was bath applied for 10 min during which TBS was delivered to both pathways. Below, representative field potential recordings.

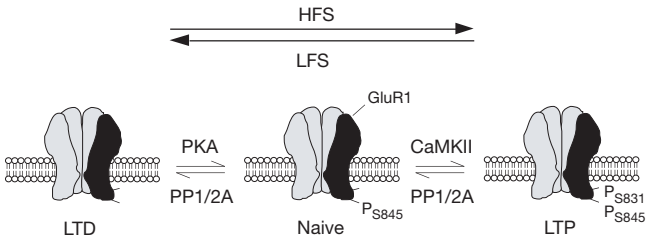

Figure 5 A model explaining the bidirectional changes in AMPA-receptor phosphorylation and NMDA-receptor-dependent synaptic plasticity. High-frequency stimulation (HFS) delivered to naive synapses preferentially activates CaMKII, which increases phosphorylation of GluR1 on Ser 831 (CaMKII site; P_{831}) resulting in LTP. In contrast, low frequency stimulation (LFS) given in a naive slice activates protein phosphatases (including PP1/2A), which dephosphorylate Ser 845 (PKA site; P_{845}). However, LFS given to a previously potentiated synapse (LTP) dephosphorylates Ser 831, as shown in our depotentiation result. On the other hand, HFS delivered to previously depressed synapses (LTD) phosphorylates Ser 845, as shown by our de-depression data.

To examine de-depression, we induced LTD in two slices in the recording chamber; 30 min later we delivered TBS to one of the slices. The synaptic response in slices that received TBS was potentiated back to around the baseline response (110 ± 4% of baseline, $n = 10$; Fig. 3d) whereas the synaptic strength in slices that only received LFS stayed depressed throughout the experiment (81 ± 4% of baseline; Fig. 3d). There was no significant change in phosphorylation of Ser 831 (CaMKII/PKC site) following de-depression (93 ± 6% of LTD slices, $n = 10$; Fig. 3e and f). Interestingly, the de-depression increased phosphorylation at Ser 845 (PKA site; 129 ± 9% of LTD slices; paired t-test: $P < 0.05$; Fig. 3e and f). These results indicate that, like LTD-inducing stimuli, LTP-inducing stimuli result in the differential regulation of GluR1 phosphorylation depending on the previous experience of the synapse. TBS delivered to 'naive' synapses causes phosphorylation of a CaMKII site, but TBS delivered to previously depressed synapses causes phosphorylation of a PKA site.

From these results we predict that the synaptic potentiation due to changes in AMPA receptor phosphorylation following TBS-induced de-depression or TBS-induced LTP should be differentially sensitive to CaMKII and PKA inhibitors. To test this hypothesis, we performed two-pathway experiments in which we could directly compare, in the same slices, the effects of TBS on naive and previously depressed synaptic inputs (Fig. 4). Under control conditions, TBS produced the same amount of synaptic potentiation regardless of the initial state of the synapses ($n = 11$; Fig. 4a), and both LTP and de-depression were prevented when NMDA receptors were blocked ($n =$ Fig. 4b). However, when slices were incubated in the selective CaMKII inhibitor KN-93 (10 μM in 0.1% DMSO), TBS produced significantly less *de novo* potentiation than de-depression (measured 50 min after TBS; $P < 0.02$, paired t-test; $n = 8$; Fig. 4c). Conversely, when PKA was transiently inhibited at the time of tetanic stimulation using the selective inhibitor KT5720 (1 μM in 0.1% DMSO), TBS produced significantly less de-depression than *de novo* LTP (measured 50 min after TBS; $P < 0.02$, paired t-test; $n = 6$; Fig. 4d). Thus, the relative contributions of CaMKII and PKA to TBS-induced potentiation vary depending on the initial state of the synapse, as predicted. This conclusion agrees with a previous report suggesting that there are different LTP-expression mechanisms in naive versus depressed synapses in PKC-γ knockout mice[23].

Our results show that bidirectional changes in synaptic function are associated with the reversible regulation of AMPA receptor phosphorylation. However, the phosphorylation or dephosphorylation of GluR1 occurred on distinct sites, depending on the past experience of the synapse (Fig. 5). Although the mechanism of this differential phosphorylation remains to be determined, it may involve differential activation of protein kinases and protein phosphatases in the potentiated, naive and depressed synapses. This differential bidirectional regulation of the phosphorylation of AMPA receptors has significant computational implications for synaptic plasticity, as the results indicate that there may be at least three states of AMPA receptor activity with limited and regulated transitions between the states.

Although phosphorylation of the GluR1 subunit on either Ser 831 or Ser 845 potentiates AMPA receptor function, it appears to do so through distinct biophysical mechanisms[15,16]. PKA phosphorylation of Ser 845 regulates the open channel probability of AMPA receptors[16], whereas CaMKII phosphorylation regulates the apparent single-channel conductance of the receptor[15]. Note that single-channel conductance increases with LTP[24]. Regulation of phosphorylation at these two sites should contribute to the changes in the efficacy of synaptic transmission that are observed during LTP and LTD. However, the trafficking and synaptic targeting of AMPA receptors may also be important in LTP and LTD[25,26]. The role of phosphorylation of the GluR1 subunit in the regulation of AMPA receptor synaptic targeting is unclear. It is possible that phosphorylation of these sites regulates synaptic trafficking of the AMPA receptor in addition to regulating channel function. Alternatively, the synaptic trafficking of AMPA receptors may be regulated through a distinct mechanism, occurring with and complementing the modification of channel properties. Our findings that different phosphorylation sites and signal-transduction pathways contribute to bidirectional synaptic modifications in the hippocampus provide evidence for unexpected complexity in the control of the gain of excitatory synaptic transmission. □

Methods

Slice preparation

We prepared hippocampal slices from postnatal day 21–30 male Long–Evans rats (Harlan) as described[6]. In brief, dissection was done using ice-cold dissection buffer (composition in mM: sucrose, 212.7; KCl, 2.6; NaH_2PO_4, 1.23; $NaHCO_3$, 26; dextrose, 10; $MgCl_2$, 3; $CaCl_2$, 1) bubbled with 95% O_2/5% CO_2. A block of hippocampus was removed and sectioned into 400-μm-thick slices using a vibratome. Area CA3 was surgically removed after sectioning. The slices were transferred to a submersion-type holding chamber containing artificial cerebrospinal fluid (ACSF; in mM: NaCl, 124; KCl, 5; NaH_2PO_4, 1.25; $NaHCO_3$, 26; dextrose, 10; $MgCl_2$, 1.5; $CaCl_2$, 2.5) bubbled with 95% O_2/5% CO_2 and equilibrated at room temperature for about 1 h. Slices were then transferred to a submersion-type recording chamber continually perfused with 29–30 °C oxygenated ACSF at 2 ml min^{-1}. For the experiments shown in Fig. 4, 500-μm-thick hippocampal slices were used and the ACSF composition included 1 mM $MgCl_2$ and 2 mM $CaCl_2$.

Electrophysiological recordings

In most cases, we recorded from two slices simultaneously in the same recording chamber. We evoked synaptic responses by stimulating Schaffer collaterals with 0.2-ms pulses delivered using concentric bipolar stimulating electrodes (FHC), and recorded them extracellularly in CA1 stratum radiatum. Baseline responses were obtained by stimulating at 0.033 Hz using an intensity that yielded a half-maximal field potential slope. To induce LTP, four episodes of TBS were delivered at 0.1 Hz, using the same stimulation intensity as for baseline. TBS consists of 10 stimulus trains delivered at 5 Hz with each train consisting of four pulses at 100 Hz. Homosynaptic LTD was induced by delivering LFS (900 pulses at 1 Hz) at the same stimulation intensity as baseline[27]. After the recording, slices were quickly frozen on dry ice for immunoblot analysis.

For two-pathway experiments, two stimulating electrodes were placed on either side of the recording field potential electrode to stimulate two independent synaptic inputs, alternating every 15 s. The absence of cross-pathway paired-pulse facilitation was used to ensure that the two inputs were independent of each other. KN-93 (Calbiochem) was dissolved in 100% DMSO (Sigma) and directly applied to the ACSF perfusion solution to reach a final concentration of 10 μM in 0.1% DMSO.

Preparation of slices for SDS–PAGE

Homogenates of hippocampal slices were prepared by sonicating each slice on ice in 1 ml of resuspension buffer (10 mM sodium phosphate (pH 7.0), 100 mM NaCl, 10 mM sodium pyrophosphate, 50 mM NaF, 1 mM sodium orthovanadate, 5 mM EDTA, 5 mM EGTA, 1 μM okadaic acid and 10 U ml^{-1} aprotinin) for 20 s. The homogenates were centrifuged at 14,000*g* for 10 min at 4 °C. The crude membrane pellets were resuspended in SDS sample buffer and loaded onto SDS–PAGE gels (7.5%). We usually loaded a control sample of hippocampus onto each gel at different protein concentrations to confirm that the protein concentration in our samples falls in the linear range of antibody detection. The resulting gels were transferred to PVDF membranes.

Immunoblot analysis

The phosphorylation-site-specific antibodies were generated and purified as described[14]. PVDF membranes were incubated in 25% methanol and 10% acetic acid (15 min). The membranes were then blocked with 1% BSA and 0.1% Tween-20 in PBS for 1 h, incubated for 1–2 h with the phosphorylation-site-specific antibodies (150–500 mg ml^{-1} in blocking buffer), washed five times for 5 min with blocking buffer, and incubated for 1 h with alkaline phosphatase-conjugated anti-rabbit immunoglobulin (1:10,000 in blocking buffer). After final washes in blocking buffer (5 × 5 min) the membranes were immersed in chemifluorescence (ECF) substrate (Amersham) for 5–30 min. The membranes were dried between filter papers, and scanned in Storm 860 (Molecular Dynamics) at 750–900 V. The phosphorylation-site-specific antibodies were stripped from the membranes by incubation in 62.5 mM Tris (pH 6.8), 2% SDS and 0.7% 2-mercapto-ethanol at 60 °C for 20 min; the membranes were then reprobed with anti-GluR1 C-terminal antibodies to estimate the total amount of GluR1. The scanned digital images were quantified using ImageQuant software (Molecular Dynamics). We analysed the relative amount of GluR1 phosphorylation by determining the ratio of the signals (P/C ratio) detected using the phosphorylation-site-specific antibodies (P) and the phosphorylation-independent C-terminal antibody (C). The P/C ratio of the control and the matching test slices was used for statistical analysis. For display purposes, this ratio was normalized to the control to derive the percentage of control values. The linearity of immunoblots was confirmed by analysing the ratio of the control samples loaded at different concentrations on each gel. The ECF method gives a better linear signal than conventional chemiluminescence (ECL) detection when looking at the ratio of signals.

Received 20 March; accepted 24 April 2000.

1. Bliss, T. V. P. & Collingridge, G. L. A synaptic model of memory: long-term potentiation in the hippocampus. *Nature* **361,** 31–39 (1993).
2. Bear, M. F. & Abraham, W. C. Long-term depression in hippocampus. *Annu. Rev. Neurosci.* **19,** 437–462 (1996).
3. Bear, M. F. A synaptic basis for memory storage in the cerebral cortex. *Proc. Natl Acad. Sci. USA* **93,** 13453–13459 (1996).
4. Malenka, R. C. & Nicoll, R. A. Long-term potentiation—a decade of progress? *Science* **285,** 1870–1874 (1999).
5. Barria, A., Muller, D., Derkach, V., Griffith, L. C. & Soderling, T. R. Regulatory phosphorylation of AMPA-type glutamate receptors by CaM-KII during long-term potentiation. *Science* **276,** 2042–2045 (1997).
6. Lee, H. -K., Kameyama, K., Huganir, R. L. & Bear, M. F. NMDA induces long-term synaptic depression and dephosphorylation of the GluR1 subunit of AMPA receptors in hippocampus. *Neuron* **21,** 1151–1162 (1998).
7. Kameyama, K., Lee, H. -K., Bear, M. F. & Huganir, R. L. Involvement of a postsynaptic protein kinase A substrate in the expression of homosynaptic long-term depression. *Neuron* **21,** 1163–1175 (1998).
8. Hollmann, M. & Heinemann, S. Cloned glutamate receptors. *Annu. Rev. Neurosci.* **17,** 31–108 (1994).
9. Seeburg, P. H. The molecular biology of mammalian glutamate receptor channels. *Trends Neurosci.* **16,** 359–365 (1993).
10. Squire, L. R. Memory and the hippocampus: A synthesis from findings with rats, monkeys, and humans. *Psychol. Rev.* **99,** 195–231 (1992).
11. Zamanillo, D. *et al.* Importance of AMPA receptors for hippocampal synaptic plasticity but not for spatial learning. *Science* **284,** 1805–1811 (1999).
12. Roche, K. W., O'Brien, R. J., Mammen, A. L., Bernhardt, J. & Huganir, R. L. Characterization of multiple phosphorylation sites on the AMPA receptor GluR1 subunit. *Neuron* **16,** 1179–1188 (1996).
13. Barria, A., Derkach, V. & Soderling, T. Identification of the Ca^{2+}/calmodulin-dependent protein kinase II regulatory phosphorylation site in the α-amino-3-hydroxyl-5-methyl-4-isoxazole-propionate type glutamate receptor. *J. Biol. Chem.* **272,** 32727–32730 (1997).
14. Mammen, A. L., Kameyame, K., Roche, K. W. & Huganir, R. L. Phosphorylation of the α-amino-3-hydroxy-5-methylisoxazole-4-propionic acid receptor GluR1 subunit by calcium/calmodulin-dependent kinase II. *J. Biol. Chem.* **272,** 32528–32533 (1997).
15. Derkach, V., Barria, A. & Soderling, T. R. Ca^{2+}/calmodulin-kinase II enhances channel conductance of alpha-amino-3-hydroxy-5-methyl-4-isoxazolepropionate type glutamate receptors. *Proc. Natl Acad. Sci. USA* **96,** 3269–3274 (1999).
16. Banke, T. B. *et al.* Control of GLuR1 AMPA receptor function by cAMP-dependent protein kinase. *J. Neurosci.* **20,** 89–102 (2000).
17. Mulkey, R. M., Herron, C. E. & Malenka, R. C. An essential role for protein phosphatases in hippocampal long-term depression. *Science* **261,** 1051–1055 (1993).
18. Mulkey, R. M., Endo, S., Shenolikar, S. & Malenka, R. C. Involvement of a calcineurin/inhibitor-1 phosphatase cascade in hippocampal long-term depression. *Nature* **369,** 486–488 (1994).
19. Malenka, R. C. *et al.* Long-term potentiation: an essential role for postsynaptic calmodulin and protein kinase activity. *Nature* **340,** 554–557 (1989).
20. Malinow, R., Schulman, H. & Tsien, R. W. Inhibition of postsynaptic PKC or CaMKII blocks induction but not expression of LTP. *Science* **245,** 862–866 (1989).
21. Lledo, P.-M. *et al.* Calcium/calmodulin-dependent kinase II and long-term potentiation enhance synaptic transmission by the same mechanism. *Proc. Natl Acad. Sci. USA* **92,** 11175–11179 (1995).
22. Otmakhov, N., Griffith, L. C. & Lisman, J. E. Postsynaptic inhibitors of calcium/calmodulin-dependent protein kinase type II block induction but not maintenance of pairing-induced long-term potentiation. *J. Neurosci.* **17,** 5357–5365 (1997).
23. Abeliovich, A. *et al.* Modified hippocampal long-term potentiation in PKC gamma-mutant mice. *Cell* **75,** 1253–1262 (1993).
24. Benke, T. A., Luthi, A., Isaac, J. T. & Collingridge, G. L. Modulation of AMPA receptor unitary conductance by synaptic activity. *Nature* **393,** 793–797 (1998).
25. Carroll, R. C., Lissing, D. V., von Zastrow, M., Nicoll, R. A. & Malenka, R. C. Rapid redistribution of glutamate receptors contributes to long-term depression in hippocampal cultures. *Nature Neurosci.* **2,** 454–460 (1999).
26. Shi, S. H. *et al.* Rapid spine delivery and redistribution of AMPA receptors after synaptic NMDA receptor activation. *Science* **284,** 1811–1816 (1999).
27. Dudek, S. M. & Bear, M. F. Homosynaptic long-term depression in area CA1 of hippocampus and the effects of NMDA receptor blockade. *Proc. Natl Acad. Sci. USA* **89,** 4363–4367 (1992).

Acknowledgements

We thank C. Doherty for help in preparing the antibodies and D. Bury for help with the manuscript. This work was supported by the Howard Hughes Medical Institute, NARSAD and The Grable Foundation.

Correspondence and requests for materials should be addressed to R.L.H. (e-mail: rhuganir@jhmi.edu).

Stable germline transformation of the malaria mosquito *Anopheles stephensi*

Flaminia Catteruccia*†, Tony Nolan*†, Thanasis G. Loukeris‡, Claudia Blass‡, Charalambos Savakis§, Fotis C. Kafatos‡ & Andrea Crisanti*

* *Imperial College of Science, Technology and Medicine, Imperial College Road, London SW7 2AZ, UK*
‡ *European Molecular Biology Laboratory, Meyerhofstrasse 1, 69117 Heidelberg, Germany*
§ *Institute of Molecular Biology and Biotechnology, Research Centre of Crete, Foundation for Research and Technology Hellas, Heraklion, Crete, Greece*
† *These authors contributed equally to this work*

Anopheline mosquito species are obligatory vectors for human malaria, an infectious disease that affects hundreds of millions of people living in tropical and subtropical countries. The lack of a suitable gene transfer technology for these mosquitoes has hampered the molecular genetic analysis of their physiology, including the molecular interactions between the vector and the malaria parasite. Here we show that a transposon, based on the *Minos* element[1] and bearing exogenous DNA, can integrate efficiently and stably into the germ line of the human malaria vector *Anopheles stephensi*, through a transposase-mediated process.

Genetic and genomic information on malaria vectors has expanded substantially during the last few years. However, further progress is hampered by the lack of germline transformation, a key technology in functional studies. In the fruitfly *Drosophila melanogaster* the development of gene transfer techniques has promoted, in a short time, a large flow of functional information on genes involved in embryogenesis, tissue modelling, intracellular signalling, neuronal organisation, behaviour and innate immunity. This success has prompted the development of methods for introducing